British Journal of Pharmacology

British Journal of Pharmacology (2018) **175** 3504–3515 3504

RESEARCH PAPER

Drug resistance profiles of mutations in the RET kinase domain

Correspondence Jie Wu, PhD, Peggy and Charles Stephenson Cancer Center, University of Oklahoma Health Sciences Center, 975 NE 10th Street, BRC-413, Oklahoma City, OK 73104, USA. E-mail: jie-wu@ouhsc.edu

Received 21 January 2018; **Revised** 25 May 2018; **Accepted** 5 June 2018

Xuan Liu[1,2,*], Tao Shen[1,2,*], Blaine H M Mooers[1,3], Frank Hilberg[4] and Jie Wu[1,2]

[1]Peggy and Charles Stephenson Cancer Center, University of Oklahoma Health Sciences Center, Oklahoma City, OK, USA, [2]Department of Pathology, University of Oklahoma Health Sciences Center, Oklahoma City, OK, USA, [3]Department of Biochemistry and Molecular Biology, University of Oklahoma Health Sciences Center, Oklahoma City, OK, USA, and [4]Department of Pharmacology, Boehringer Ingelheim RCV GmbH & Co KG, Vienna, Austria

*Equal contributing authors.

BACKGROUND AND PURPOSE

Alterations in the tyrosine kinase enzyme RET are found in thyroid and lung cancer. While RET TK inhibitors (TKIs) are used to treat thyroid cancer and are in clinical trials for RET fusion-positive non-small cell lung cancer, the impact of mutations in the RET kinase domain on drug sensitivity is largely uncharacterized.

EXPERIMENTAL APPROACH

We identified and analysed mutations in the RET kinase domain that conferred resistance to the TKIs cabozantinib, lenvatinib, vandetanib and nintedanib using RET kinase-dependent BaF3/KIF5B-RET (BaF3/KR) cells. We also examined the sensitivity of RET (M918T), a RET mutation prevalent in aggressive multiple endocrine neoplasia type 2B, to these TKIs in the context of BaF3/KR cells.

KEY RESULTS

Fourteen mutations were analysed. Pan resistance to the four TKIs was found in six RET kinase domain mutations (L730I, V738A, V804L/M, Y806N, G810S). Seven RET kinase domain mutations (L730V, E732K, A807V, G810A, V871I, M918T, F998V) displayed selective resistance to one or more of these drugs. L730I/V and G810A/S had different drug resistance profiles. V871I, M918T and F998V mutations are located at distant sites away from the TKI binding pocket.

CONCLUSIONS AND IMPLICATIONS

A panel of TKI-resistant RET mutations were identified, and their drug sensitivities were cross-profiled. The results provide a reference for selecting appropriate TKIs to inhibit RET kinase domain mutants. Besides changes in the drug-interacting residues, mutations at distant sites could exert long-range effects resulting in TKI resistance. Among the four TKIs analysed here, nintedanib remained unaffected by mutations at the three distant sites.

Abbreviations

BaF3/KR, stable BaF3 cell line expression KIF5B-RET; BaF3/KRmut, stable BaF3 cell line expression KIF5B-RET mutant; FMTC, familial medullary thyroid carcinoma; MEN2, multiple endocrine neoplasia type 2; MTC, medullary thyroid carcinoma; NSCLC, non-small cell lung cancer; pRET, Tyr^{905} phosphorylated RET; PTK, protein TK; RET, rearranged during transfection; TKI, TK inhibitor

DOI:10.1111/bph.14395

Introduction

The ***RET*** proto-oncogene encodes a transmembrane protein tyrosine kinase (PTK) (Wells *et al.*, 2013; Krampitz and Norton, 2014). Missense mutations in *RET* cause multiple endocrine neoplasia type 2 (MEN2), which includes MEN2A, MEN2B and familial medullary thyroid carcinoma (FMTC). The main clinical presentation of MEN2 is medullary thyroid carcinoma (MTC). Mutations in RET found in MEN2A are located mostly at the sites of extracellular Cys residues, whereas the p.Met^{918}Thr (designated M918T) mutation in the cytoplasmic PTK domain is associated with more aggressive MEN2B and is the most frequently detected RET mutation in sporadic MTC (Kodama *et al.*, 2005; Wells *et al.*, 2013). In addition to missense point mutations, oncogenic fusions of RET are found in papillary thyroid carcinoma (PTC) (Mulligan, 2014). More recently, RET fusions have been discovered in 1–2% of non-small cell lung cancer (NSCLC) (Gainor and Shaw, 2013; Kohno *et al.*, 2013). KIF5B-RET is the most frequently occurring RET fusion in NSCLC (Kohno *et al.*, 2015). RET fusion partners in PTC and NSCLC contain a coiled-coil domain that induces dimerization and constitutive activation of the RET. RET mutants and RET fusion proteins are oncogenic as demonstrated by transformation of cells in cultures and tumourigenesis in animal models (Pasini *et al.*, 1997; Takeuchi *et al.*, 2012; Huang *et al.*, 2016).

Cabozantinib, **lenvatinib** and **vandetanib** are multi-kinase, protein tyrosine kinase inhibitors (TKIs) that selectively inhibit **VEGFR-2**, RET and a few other PTKs such as **MET**, **KIT**, FGF receptor **FGFR1** and **PDGFRs**, depending on the inhibitors. Cabozantinib and vandetanib have been approved to treat advanced and metastatic MTC, whereas lenvatinib is approved to treat recurrent, metastatic, progressive, radioactive iodine-refractory differentiated thyroid cancer (Mulligan, 2014; Mulligan, 2016). Earlier trials of these drugs in thyroid cancer showed that patients treated with these TKIs had increased progression-free survival (PFS) (Wells *et al.*, 2012; Elisei *et al.*, 2013; Schlumberger *et al.*, 2015). More recent clinical studies of cabozantinib in MTC have found that the drug increased overall survival (Mulligan, 2016) and that the RET mutation-positive cohort of MTC patients had the best PFS benefits from the cabozantinib treatment (Sherman *et al.*, 2016). This finding suggests that MTC has oncogene addiction to the mutated *RET* gene. Nevertheless, as we will present in this study, a higher concentration of cabozantinib is required to inhibit the RET (M918T) mutant kinase. Thus, the best possible clinical benefit of targeting RET in MTC may not have been achieved. The oncogenic RET fusion kinase has also been targeted in ongoing clinical trials in NSCLC with cabozantinib, lenvatinib and vandetanib (Kohno *et al.*, 2013). While the low rate of RET fusions in NSCLC has limited the progress of prospective clinical trials, objective response rates range from 16 to 53% in small phase II trials of cabozantinib and vandetanib and a multiple centre clinical data analysis (Drilon *et al.*, 2016; Gautschi *et al.*, 2017; Yoh *et al.*, 2017).

Targeted cancer therapy with TKIs is subject to intrinsic and acquired resistance. In **EGFR**- and anaplastic lymphoma kinase (**ALK**)-targeted therapies in EGFR mutation-positive and ALK fusion-positive NSCLC, a common mechanism of acquired TKI resistance is secondary mutations in the kinase domains that sterically block the binding of TKIs (Katayama *et al.*, 2012; Katayama *et al.*, 2015; Riely and Yu, 2015). At least some of these drug-resistant EGFR and ALK mutants have been successfully inhibited by second and third generations of EGFR or ALK TKIs such as the EGFR inhibitor **osimertinib** (Cross *et al.*, 2014), or ALK inhibitors **alectinib**, **ceritinib** (Katayama *et al.*, 2015), **lorlatinib** (Johnson *et al.*, 2014; Zou *et al.*, 2015) and **brigatinib** (Sabari *et al.*, 2017).

Because some MTC-associated sites of mutations are located in the cytoplasmic PTK domain of RET, it is important to know whether these mutations affect drug sensitivity. Aside from the gatekeeper V804 mutations (Huang *et al.*, 2016), the impact of other PTK domain mutations on drug sensitivity is mostly unknown. In NSCLC, RET fusion-targeted TKI treatment may also lead to acquired resistance due to secondary mutations in the RET kinase domain. An advantage of RET-targeted therapy is that several RET inhibitors have already been identified (Gild *et al.*, 2011; Song, 2015). Because these TKIs have different chemical structures, a mutation in the RET kinase domain may only induce resistance to a subset of these TKIs, so that other RET TKIs may be used to inhibit the activity of the mutant RET kinase.

Because cabozantinib, lenvatinib and vandetanib were approved to treat advanced and metastatic MTC and were in clinical trials of RET fusion-positive NSCLC (Kohno *et al.*, 2013), we used a random mutagenesis drug resistance selection method to find mutant RETs that conferred resistance to these TKIs. We also identified **nintedanib** as a potent RET inhibitor and found two nintedanib-resistant RET mutations through long-term culture of KIF5B-RET-dependent cells in medium containing nintedanib. The sensitivities of these RET mutations, two RET mutations identified in a previous study (Huang *et al.*, 2016) and the MEN2B-associated RET (M918T) mutation, were then cross-profiled against these four TKIs to reveal their drug resistance/sensitivity profiles.

Methods

Random mutagenesis

To generate a pool of random mutations of KIF5B-RET, a lentiviral plasmid encoding KIF5B-RET (pLentP-KR, 1 μg) (Huang *et al.*, 2016) was transformed into 100 μL of XL1-Red competent cells and plated onto ten 10 cm lysogeny broth/ampicillin agar plates, which yielded >50 000 colonies. Plasmid DNA was prepared from the pool of ampicillin-resistant XL1-Red bacteria. One-tenth of DNA was amplified in Stbl3 bacteria. Then 2% of the amplified DNA was used to generate lentiviruses encoding the KIF5B-RET mutation pool by co-transfection of 293T cells with pLentP-KR mutation pool DNA, psPAX2 and pMD2.G using lipofectamine 3000.

Identification of drug-resistant mutations from the random mutation pool

BaF3 cells (1×10^7 cells) (Huang *et al.*, 2016) were cultured in RPMI-1640/10% FBS/1 ng·mL^{-1} mouse **IL-3** and infected with the lentiviruses prepared above. Infected cells were selected with puromycin (1 μg·mL^{-1}) for 2 weeks in RPMI-1640/10% FBS/1 ng·mL^{-1} IL-3 medium. Next, puromycin-

resistant cells were cultured in IL-3-free medium for 1 week to select IL-3-independent cells. The puromycin-resistant, IL-3-independent cells were divided into three portions and then cultured in semi-solid MethoCult H4100 methylcellulose cultures (Stemcell Technologies, Cambridge, MA, USA) in RPMI-1640/10% FBS in the presence of cabozantinib (1.0 μM), lenvatinib (1.3 μM) or vandetanib (4.0 μM). These drug concentrations were ~5-fold of previously determined IC_{50} concentrations (Huang *et al.*, 2016). Colonies of drug-resistant cells were isolated, and the cells were expanded in RPMI-1640/10% FBS medium. Genomic DNA was prepared from individual cell lines. Both strands of the human RET kinase domain in the KIF5B-RET cDNA construct were sequenced. The RET amino-acid sequence numbering was based on the GenPept entry NP_066124.

Identification of nintedanib-resistant mutations

Ten T-75 flasks of BaF3/KR cells (2×10^7 cells per flask) were cultured in RPMI-1640/10% FBS medium plus stepwise increased concentrations of nintedanib at 0.2, 0.4, 0.8, 1.6, 2.4 and 3.2 μM over the course of 4 months. Genomic DNA were isolated from the surviving cells starting at 0.4 μM nintedanib, and the KIF5B-RET kinase domain-coding region was sequenced to examine mutation(s). After identification of drug-resistant mutations, KIF5B-RET plasmid constructs containing the mutations were made by replacement with restriction fragments containing the mutations. BaF3/KRmut cells were made from lentiviruses encoding the mutated KIF5B-RET and were used to validate the drug resistance of these mutants and to profile their sensitivity to TKIs.

Cell lines, drug sensitivity assay and immunoblotting

BaF3 cell lines containing mutations in the KIF5B-RET kinase domain used in inhibitor profiling were recreated by infecting BaF3 cells with lentiviruses containing individual RET mutations. Briefly, a KIF5B-RET cDNA containing an identified RET mutation was generated by replacing the KIF5B-RET cDNA restriction fragment with the corresponding DNA fragment isolated from the BaF3 cell line harbouring that mutation. The KIF5B-RET coding sequence containing the RET (M918T) mutation was generated by site-directed mutagenesis using PCR. The KIF5B-RET mutation cDNA was then subcloned into a lentiviral plasmid (pLentP). Lentiviruses were then prepared and used to infect BaF3 cells. The infected cells were selected by culturing them in RPMI-1640/10% FBS plus 1 $ng \cdot mL^{-1}$ puromycin in the absence of IL-3.

The cell viability assay was performed using CellTiter-Glo reagent (Promega, Madison, WI, USA) as described previously (Huang *et al.*, 2016), except that viable cells were measured 3 days after drug treatment. IC_{50} data of BaF3/KR and BaF3/KRmut cells were from five to seven experiments performed in two or three technical replicates. For immunoblotting analysis of RET, cells were treated with a drug for 4 h at the concentrations indicated in the figure legends. Cell lysate preparation and analysis by immunoblotting were performed as described previously (Huang *et al.*, 2016; Shen *et al.*, 2017). Results of immunoblots were confirmed in independent experiments.

In vitro kinase assay

In vitro IC_{50} values were determined by a contract service (Reaction Biology, Malvern, PA, USA) using affinity-purified recombinant RET kinase domain proteins (amino-acid residues 658–1114 of RET with N-terminal GST tag) produced by baculoviruses in insect cells and a 10-dose IC_{50} assay. The reaction mixture contained 20 mM HEPES, pH 7.5, 10 mM $MaCl_2$, 1 mM EGTA, 0.02% Brij35, 0.02 $mg \cdot mL^{-1}$ BSA, 0.1 mM Na_3VO_4, 2 mM DTT, 1% DMSO, 10 μM [^{32}P]-ATP and 20 μM CHKtide (KKKVSRSGLYRSPSMPENLNRPR), plus recombinant RET proteins. Phosphorylated peptide was detected by a filter-binding method. Kinase activity was expressed as the % remaining kinase activity in test samples compared with vehicle (DMSO) reactions.

Flow cytometric analysis

BaF3/KR and BaF3/KR (E732K) cells (2×10^5 cells each) were cultured in RPMI-1640/10% FBS medium and treated with vehicle or the indicated TKI (0.3 μM) for 48 h. After drug treatment, cells were washed in cold PBS and then processed for binding to FITC-conjugated annexin V/propidium iodide using the FITC Annexin V/Dead Cell Apopotosis Kit (Invitrogen, Waltham, MA, USA) according to the manufacturer's instructions. Stained cells were analysed using a Stratedigm S1000 flow cytometer ($n = 6$).

Molecular modelling

The programme PyMOL (Schrodinger LLC, Cambridge, MA, USA) was used to examine the RET-vandetanib co-crystal structure (PDB: 2ivu) (Knowles *et al.*, 2006) and to prepare the molecular artwork.

Data analysis

Curve fitting was performed as described previously (Scott *et al.*, 2011) using the GraphPad Prism 6 software to obtain the IC_{50} values and 95% confidence intervals of the IC_{50} value. Comparison of IC_{50} values or apoptotic cells in flow cytometric analysis was performed using Student's unpaired *t*-test with Welch's correction. A difference in IC_{50} values with $P < 0.05$ was considered statistically significant. The data and statistical analysis comply with the recommendations on experimental design and analysis in pharmacology (Curtis *et al.*, 2018).

Materials

XL1-Red competent cells were obtained from Agilent (Santa Clara, CA, USA). Mouse IL-3 was purchased from PeproTech (Rocky Hill, NJ, USA). Cabozantinib, lenvatinib and vandetanib were procured from LC Laboratories (Woburn, MA, USA). Nintedanib was either obtained from LC laboratories or provided by Boehringer Ingelheim (Vienna, Austria).

Nomenclature of targets and ligands

Key protein targets and ligands in this article are hyperlinked to corresponding entries in http://www.guidetopharmacology.org, the common portal for data from the IUPHAR/BPS Guide to PHARMACOLOGY (Harding *et al.*, 2018), and are permanently archived in the Concise Guide to PHARMACOLOGY 2017/18 (Alexander *et al.*, 2017).

Results

Identification of TKI-resistant RET kinase mutations

To discover TKI-resistant RET mutations, we used an *Escherichia coli* strain (XL1-Red) deficient in DNA repair to generate a pool of random mutations of KIF5B-RET cDNA. We then expressed a sample of this cDNA pool in BaF3 cells and selected TKI-resistant cells by culturing the lentivirus-infected BaF3 cells in IL-3-free medium with the selected drugs. BaF3 cells depend on IL-3 for cell survival and proliferation. KIF5B-RET can confer BaF3 cells to survive and grow independently of IL-3, but this requires RET PTK activity (Huang *et al.*, 2016). Thus, BaF3 cells expressing KIF5B-RET (BaF3/KR) provide an excellent cell model for identification of RET TKI-resistant mutations (Huang *et al.*, 2016). DNA was prepared from each of TKI-resistant BaF3/KRmut cells, and the RET kinase domain coding sequence was analysed to identify TKI-resistant mutations.

Cabozantinib, lenvatinib and vandetanib have been approved by the United States Food and Drug Administration (FDA) for treating advanced and metastatic thyroid cancer (Mulligan, 2014; Schlumberger *et al.*, 2015). These three drugs were also used in clinical studies of RET fusion-positive NSCLC (Kohno *et al.*, 2013). Thus, we focused on identifying mutations resistant to these three TKIs.

We used ~5-fold of previously determined IC_{50} concentrations of cabozantinib, lenvatinib or vandetanib (Huang *et al.*, 2016) to select drug-resistant cell colonies in semi-solid methylcellulose cultures. Eighty-six drug-resistant cell colonies were isolated from the semi-solid cell cultures and expanded into cell lines. Genomic DNA was prepared from each cell line, and the coding region of the KIF5B-RET kinase domain was sequenced to identify mutations. As shown in Table 1, 55 cell lines had mutations at nine sites in the RET kinase domain. The double mutant G810S/G949R was found in two vandetanib-resistant cell lines (in both cell lines, the double mutations occurred in *cis*), while the remaining resistant cell lines had single-site mutations. Thirty-one cabozantinib-resistant cell lines did not have mutation in the KIF5B-RET kinase domain. The RET kinase mutation-independent mechanism of cabozantinib resistance was not further investigated. Of note, in a previous study, we also isolated BaF3/KR cell line resistance to vandetanib that did not have mutation in the RET kinase domain (Huang *et al.*, 2016).

To confirm that these point mutations in the RET kinase domain cause TKI resistance, we reconstructed lentiviruses encoding each of the single-site mutations in KIF5B-RET (Supporting Information Figure S1). BaF3 cells were infected with this panel of lentiviruses that encode mutations at single sites in the KIF5B-RET kinase domain. The re-established BaF3/KRmut cell lines were then assayed for sensitivities to cabozantinib, lenvatinib and vandetanib, respectively. We designated drug resistance as a ≥2-fold increased IC_{50} with a $P < 0.05$. This is because the drug response curves of BaF3/KR cells were nearly symmetrical and 2× IC_{50} resulted in >90% inhibition of BaF3/KR cells in our assays (Figure 1). As presented in Table 2, the results showed that L730I, E732K and V871I mutations were resistant to cabozantinib. V738A, A807V and F998V were resistant to lenvatinib. G810S was resistant to vandetanib. Y806N was resistant to all three TKIs used in the drug-resistant mutation selection. The G949R mutation was identified as G810S/G949R double mutations. The G810S mutation was sufficient to confer vandetanib resistance, and the BaF3/KR (G810S/G949R) cell lines had similar sensitivity to vandetanib as BaF3/KR (G810S) cells (Supporting Information Figure S2). Because of this and because it would be somewhat difficult to recreate the G810S/G949R double mutants due to the lack of an appropriate restriction site for subcloning, we did not recreate the G810S/G949R double mutations or further evaluate the drug resistance of the G949R mutation. Thus, the eight evaluated RET kinase point mutations were all confirmed as conferring drug resistance to the specific TKI that was used to identify them.

Table 1

Drug-resistant mutation counts in BaF3/KRmut cell lines

	Protein TK inhibitor			
Mutation	**CBT**	**LVT**	**VDT**	**Total**
L730I	2	–	–	2
E732K	1	–	–	1
V738A	–	3	–	3
Y806N	2	22	19	43
A807V	–	1	–	1
G810S	–	–	1	1
V871I	1	–	–	1
F998V	–	1	–	1
G810S/G949R	–	–	2	2
No mutation	31	–	–	31
Total mutations	6	27	22	55
Total cell lines	37	27	22	86

CBT, cabozantinib; LVT, lenvatinib; VDT, vandetanib.

Drug-resistant KIF5B-RET mutant kinases resist TKI inhibition

RET Tyr-905 phosphorylation (pRET) is a marker of KIF5B-RET activity (Kohno *et al.*, 2012; Huang *et al.*, 2016). To determine whether the resistance to cabozantinib, lenvatinib and vandetanib of BaF3/KRmut cells was directly related to the resistance of KIF5B-RET mutant kinases in these cells to the TKIs, we selected the two most frequently detected TKI-resistant mutants for each TKI from our random mutation pool (Table 1) and tested their sensitivities to the corresponding TKI. The IC_{50}s of cabozantinib in BaF3/KR, BaF3/KR (L730I) and BaB3/KR (Y806N) cells were 0.24, 2.96 and 4.76 μM respectively (Table 2 and Figure 1A). pRET immunoblotting analysis indicated that the sensitivity to cabozantinib was KIF5B-RET > KIF5B-RET (L730I) > KIF5B-RET (Y806N) (Figure 1A). The sensitivity of pRET to lenvatinib was KIF5B-RET > KIF5B-RET (Y806N) = KIF5B-RET (V738A), which corresponded to a similar extent of resistance of BaF3/KR (Y806N) and BaF3/KR (V738A) cells to lenvatinib (IC_{50}s: 0.19 μM vs. 1.93 and 2.35 μM; Table 2 and Figure 1B). Similarly, in agreement with the similar extent of

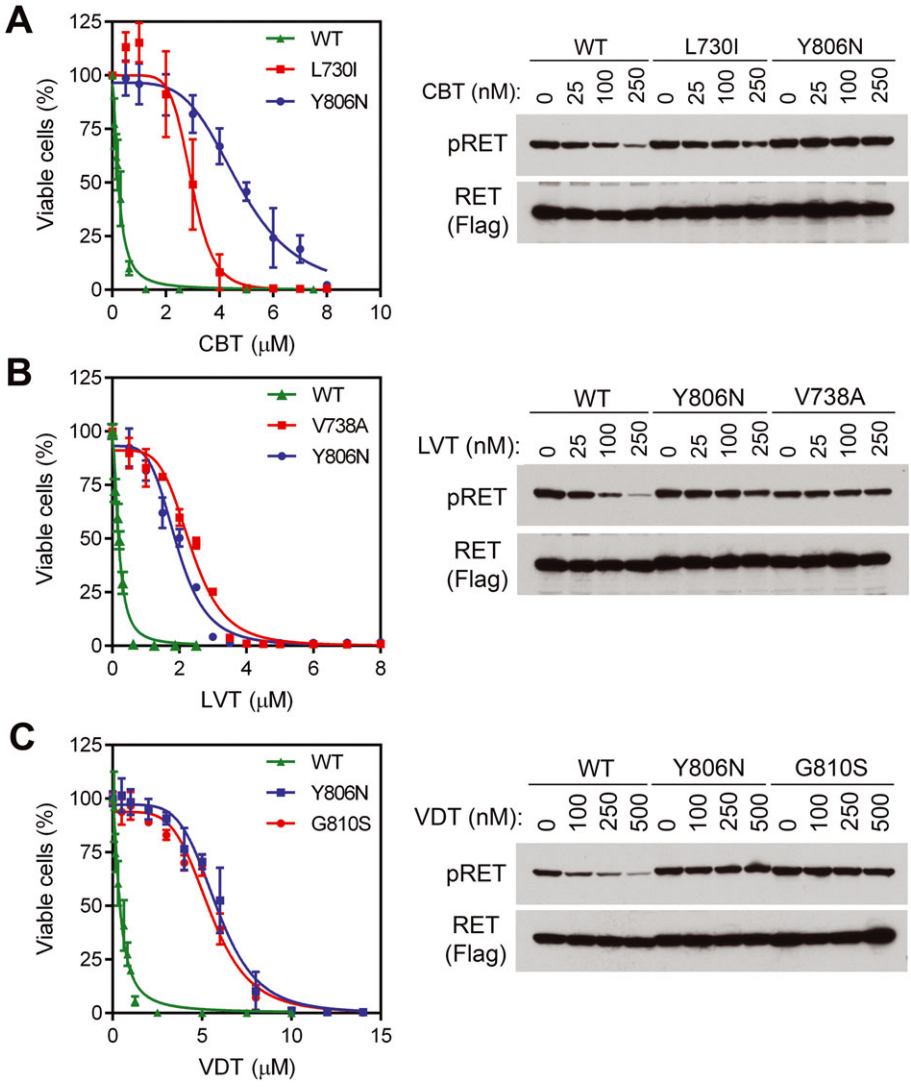

Figure 1

Dose-dependent inhibition of BaF3 cells expressing KIF5B-RET and its RET kinase domain mutants. Left panels, BaF3/KR and indicated BaF3/KRmut cells were treated with (A) cabozantinib, (B) lenvatinib or (C) vandetanib for 3 days, and the relative numbers of viable cells were determined. Right panels, cells were treated with indicated concentrations of drugs for 4 h, and cell lysates were analysed by immunoblotting with the indicated antibodies. CBT, cabozantinib; LVT, lenvatinib; VDT, vandetanib; WT, wild-type.

resistance to vandetanib of BaF3/KR (Y806N) and BaF3/KR (G810S) cells (IC_{50}s: 0.42 μM in BaF3/KR vs. 5.86 and 5.47 μM in the two cell lines with RET kinase mutations), the sensitivity of inhibiting pRET by vandetanib was KIF5B-RET > KIF5B-RET (Y806N) = KIF5B-RET (G810S) (Figure 1C).

Nintedanib is a potent RET kinase inhibitor

Nintedanib inhibits three angiokinases (VEGFR, FGFR and PDGFR) and is approved by the FDA for the treatment of idiopathic pulmonary fibrosis (Hilberg *et al.*, 2008; Roth *et al.*, 2009; Roth *et al.*, 2015). Because RET kinase inhibitors cabozantinib, lenvatinib and vandetanib are multi-kinase inhibitors with similar PTK selectivity profiles that preferentially inhibit angiokinases, we tested whether nintedanib could also inhibit RET. As shown in Figure 2A and Table 2, nintedanib inhibited the KIF5B-RET-dependent BaF3/KR cells with an IC_{50} of 0.14 μM. In the parental BaF3 cells cultured with IL-3, the IC_{50} of nintedanib was 1.64 μM (Figure 2A). Thus, an approximately 12-fold higher concentration was required for nintedanib to inhibit the IL-3-dependent BaF3 cells, demonstrating the specificity of nintedanib in inhibiting the KIF5B-RET-dependent BaF3 under IL-3-free conditions. Immunoblotting analysis of BaF3/KR cells treated with various concentrations of nintedanib detected pRET inhibition at the lowest nintedanib concentration tested (0.1 μM; Figure 2B). Consistently, *in vitro* kinase assay results showed that nintedanib inhibited recombinant RET kinase with an IC_{50} of 0.67 ± 0.22 nM (mean ± range, n = 3; Table 3 and Supporting Information Figure S3). In parallel experiments, the IC_{50}s of cabozantinib, lenvatinib and vandetanib in *in vitro* RET kinase assay were 14.7 ± 4.5, 2.8 ± 1.0 and 7.6 ± 2.0 nM (mean ± range, n = 2; Table 3) respectively. These

Table 2

TKI sensitivity profiles of RET kinase domain mutations

Mutation	IC_{50} (μM)[a]			
	Cabozantinib	Lenvatinib	Vandetanib	Nintedanib
WT	0.24 (0.21 to 0.27)	0.19 (0.18 to 0.21)	0.42 (0.35 to 0.48)	0.14 (0.13 to 0.15)
L730I	2.96 (2.80 to 3.13)	1.07 (1.03 to 1.12)	1.92 (1.79 to 2.06)	0.84 (0.81 to 0.89)
L730V	2.37 (2.28 to 2.47)	0.23 (0.21 to 0.25)	1.09 (1.04 to 1.14)	0.80 (0.77 to 0.84)
L730V/V804M	7.37 (7.21 to 7.53)	9.41 (7.93 to 10.89)	5.13 (4.89 to 5.16)	1.58 (1.48 to 1.68)
E732K	1.15 (1.08 to 1.21)	0.16 (0.15 to 0.17)	0.49 (0.44 to 0.55)	0.17 (0.16 to 0.18)
V738A	1.20 (1.16 to 1.25)	2.35 (2.26 to 2.45)	1.05 (0.95 to 1.14)	0.92 (0.86 to 0.98)
V804L	3.22 (3.00 to 3.45)	10.60 (9.19 to 12.01)	6.10 (5.82 to 6.34)	0.58 (0.51 to 0.64)
V804M	4.26 (4.01 to 4.50)	5.42 (4.92 to 5.93)	5.83 (5.57 to 6.09)	0.86 (0.80 to 0.92)
Y806N	4.76 (4.54 to 4.94)	1.93 (1.84 to 2.02)	5.86 (5.60 to 6.11)	0.91 (0.85 to 0.97)
A807V	0.57 (0.52 to 0.62)	0.54 (0.50 to 0.58)	1.05 (0.92 to 1.18)	0.12 (0.11 to 0.13)
G810A	0.22 (0.21 to 0.24)	0.11 (0.10 to 0.12)	2.76 (2.53 to 3.00)	0.13 (0.11 to 0.14)
G810S	1.05 (0.93 to 1.17)	0.67 (0.64 to 0.70)	5.47 (5.23 to 5.68)	0.56 (0.51 to 0.61)
V871I	1.07 (0.98 to 1.17)	0.52 (0.51 to 0.54)	1.00 (0.95 to 1.05)	0.18 (0.17 to 0.19)
F998V	0.74 (0.68 to 0.80)	0.87 (0.80 to 0.94)	0.77 (0.73 to 0.81)	0.14 (0.13 to 0.15)
M918T	1.57 (1.41 to 1.74)	1.42 (1.27 to 1.59)	1.83 (1.57 to 2.08)	0.24 (0.22 to 0.26)

Black: resistant; red: non-resistant.
[a]The values are mean and 95% confidence intervals.

data indicate that nintedanib is a highly potent RET kinase inhibitor. During the course of this study, nintedanib was also identified as an RET TKI by other groups (Gautschi *et al.*, 2017; Hilberg *et al.*, 2018).

To identify nintedanib-resistant RET mutations, we cultured 10 flasks of BaF3/KR cells (2×10^7 cells each) with stepwise increased concentrations of nintedanib from 0.2 to 3.2 μM. Analysis of survival cell lines identified L730V and L730V/V804M double mutations (Figure 2C, D and Supporting Information Table S1). In two cell lines (#8 and #9), the L730V mutation was found in 1.6 μM nintedanib-resistant cells, whereas L730V/V804M double mutations were found in 2.4 μM nintedanib-resistant cells (Supporting Information Table S1). Thus, KIF5B-RET evolved from the L730V single mutation to the L730V/V804M double mutation in the presence of higher concentrations of nintedanib. The L730V/V804M double mutation was observed in single cDNA clone, indicating that these two mutations occur in cis.

Sensitivity of RET kinase mutants to TKIs

In addition to the RET mutations identified above, we had previously identified RET V804L and G810A mutations (Huang *et al.*, 2016). Using the panel of these 13 KIF5B-RET-dependent BaF3/KRmut cell lines, we cross-profiled their sensitivities to cabozantinib, lenvatinib, vandetanib and nintedanib. The results are shown in Table 2.

The L730I, V738A, V804L/M, Y806N and G810S mutants were pan resistant to the four TKIs. The L730V/V804M double mutant had higher degrees of drug resistance to all four TKIs than did the L730V or V804M single-site mutant. Except for the G810A mutant, all other mutants were resistant to cabozantinib. L730V and E732K mutants and the previously reported G810A mutant were sensitive to lenvatinib, while the other mutants were resistant to lenvatinib. The cabozantinib-resistant E732K mutant was sensitive to vandetanib. The F998V mutant slightly affected (<2-fold) vandetanib sensitivity, whereas the other mutants were resistant to vandetanib. Except for the six pan-resistant mutants, the other five mutants (E732K, A807V, G810A, V871I and F998V) were sensitive to nintedanib (Table 2 and Figure 2D, E).

The TKI-resistant mutants that we identified included changes at seven sites that line the TKI binding pocket. The L730, E732 and V738 residues of the RET kinase are located in the glycine (Gly)-rich loop (L^{730}-**G**-E^{732}-**G**-E-F-**G**-K-V^{738}) of RET kinase that makes up the N-lobe wall of the TKI binding pocket (Figure 3A). L730 and V738 are conserved residues (Plaza-Menacho *et al.*, 2014). In the RET-vandetanib co-crystal structure (PDB: 2ivu), the hydrophobic side chains of L730 and V738 are close to each other and provide the upper wall of the binding pocket that packs against the quinazoline and bromofluorophenyl moieties of vandetanib (Figure 3B). The side chain of V730 makes favourable van der Waals interactions with one face of the six-membered ring of the quinazoline group that is composed of only carbon atoms. The side chain of V738 makes van der Waals contacts with one face of the terminal bromofluorophenyl ring. The side chains of V804 and Y806 make up the side wall of the binding pocket. On the underside of vandetanib, the side chain of A807 contacts the central quinazoline rings, and the side chain of V804 contacts the bromofluorophenyl ring. The mutations at these seven sites either introduced bulkier side chains that would interfere with the binding of the drug or otherwise altered the drug–protein interaction.

The side chain of E732 is exposed to the solvent; the carboxylate group of this side chain is absent in the crystal

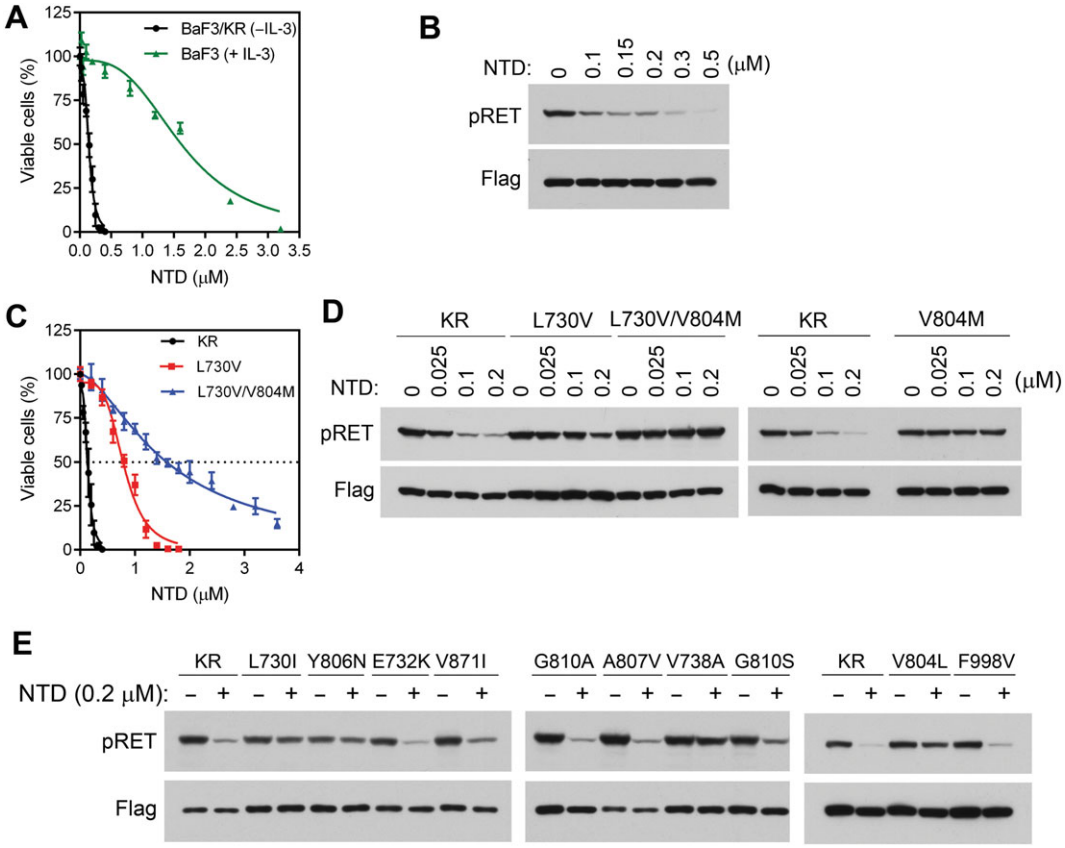

Figure 2

Analysis of effects of nintedanib in BaF3, BaF3/KR and BaF3/KRmut cells. (A) The IL-3-dependent BaF3 cells were cultured in medium containing IL-3, while the IL-3-independent BaF3/KR cells were cultured in IL-3-free medium. These cells were treated with various concentrations of nintedanib for 3 days, and relative numbers of viable cells were determined. (B) BaF3/KR cells were treated with the indicated concentrations of nintedanib for 4 h, and cell lysates were analysed by immunoblotting with the indicated antibodies. (C) Comparison of the inhibitory activities of nintedanib on BaF3/KR, BaF3/KR (L730V) and BaF3/(L730V/V804M) cells. (D and E) BaF3/KR and the indicated BaF3/KRmut cells were treated with nintedanib for 4 h at the indicated concentrations, and cell lysates were analysed by immunoblotting with the indicated antibodies. NTD, nintedanib.

Table 3

Inhibition of RET and RET (M918T) kinases *in vitro*

TKI	Experiment	IC_{50} (nM)			
		RET	RET (M918T)	Fold change (M918T per wt)	Fold change (mean ± range)
Cabozantinib	1	10.2	30.9	3.0	2.3 ± 0.7
	2	19.1	29.7	1.6	
Levatinib	1	1.8	9.7	5.4	4.4 ± 1.0
	2	3.7	12.6	3.4	
Vandetanib	1	5.6	15	2.7	2.2 ± 0.5
	2	9.5	15.6	1.6	
Nintedanib	1	0.45	0.52	1.2	1.0 ± 0.1
	2	0.89	0.77	0.9	

structure (Figure 3B). E732 is not a conserved residue in the Gly-rich loop of PTKs. E732K was identified as a cabozantinib-resistant mutation in our library of mutations (Table 1). While BaF3/KR (E732K) cells were resistant to cabozantinib, they remained sensitive to lenvatinib, vandetanib and nintedanib (Table 2). Consistently, apoptotic assays

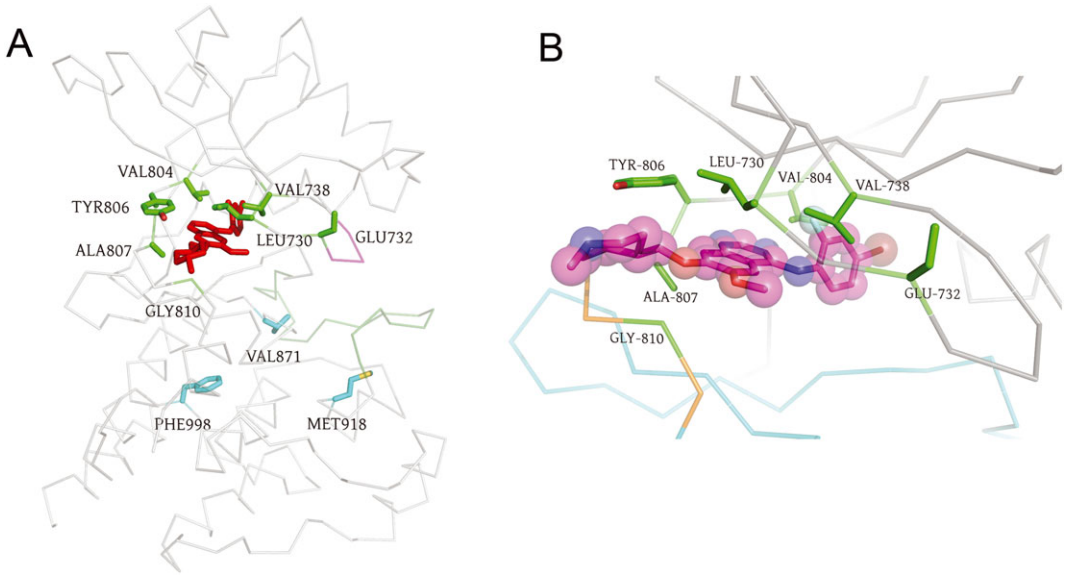

Figure 3

Structural analysis of the drug binding site in RET kinase. The crystal structure of 2iuv (Knowles *et al.*, 2006) was used to make the images. The N-lobe is at the top. The C-lobe is at the bottom. (A) C-α trace of the TK domain of RET is shown in grey. Vandetanib is shown in red as sticks. The wild-type side chains at the mutated sites are shown as sticks. Site 810 is a glycine (Gly). Mutation sites in the vandetanib binding pocket are shown in green, whereas distant mutation sites are shown in cyan. The Gly-rich loop is coloured magenta. The activation loop is coloured dark green. (B) Close up of the drug binding site. Vandetanib is shown as sticks and spheres with the carbon atoms coloured magenta, oxygen atoms coloured red, nitrogen atoms coloured blue, the fluorine atom coloured cyan and bromine atom coloured brown. N-lobe (residues 713–805) is coloured grey, the C-lobe (residues 812–1013) is coloured cyan and the intervening hinge between the two domains is coloured orange.

showed that BaF3/KR (E732K) cells were resistant to cabozantinib-induced apoptosis, whereas they were sensitive to apoptosis induced by lenvatinib, vandetanib and nintedanib (Figure 4). The RET E732 equivalent residue is a lysine in RON and an arginine in VEGFR1/2 and MET (Plaza-Menacho *et al.*, 2014), so the charge of the side chain at this solvent-accessible site is not conserved. Interestingly, the reported cabozantinib IC_{50} for RON is 124 nM, whereas the IC_{50}s for VEGFR2, MET and RET were 0.035, 1.3 and 5.3 nM respectively (Yakes *et al.*, 2011).

V804 is the gatekeeper residue in RET, while Y806, A807 and G810 are in the hinge strand connecting the N-lobe (residues 713–805) and the C-lobe (residues 812–1013) of the kinase and form the back wall of the vandetanib binding pocket (Figure 3B). Unsurprisingly, the V804L/M gatekeeper mutants were resistant to the four TKIs. Among six mutations analysed in this area, the lenvatinib-resistant mutant A807V had less effect on cabozantinib and vandetanib compared with the V804L/M, Y806N and G810S mutations and did not affect nintedanib sensitivity (Table 2). In addition to the previously identified vandetanib-resistant G810A mutation (Huang *et al.*, 2016) that blocks the entrance of the binding site, we isolated the G810S mutation. G810S mutation resulted in resistance to all four TKIs, but the smaller Ala substitution to G810 was able to accommodate cabozantinib, lenvatinib and nintedanib.

V871 and F998 are located on the C-lobe and are distant from the drug binding pocket (Figure 3A). The single-site mutants V871I and F998V were resistant to cabozantinib and lenvatinib (Table 2). The V871I mutant was resistant to vandetanib, and the F998V mutant had slightly reduced sensitivity to vandetanib. We then examined pRET levels in BaF3/KR, BaF3/KR (V871I) and BaF3/KR (F998V) cells treated with these drugs. In agreement with the results from the cell viability assay, data from the pRET immunoblotting analysis indicated that the V871I and F998V mutants were resistant to cabozantinib, lenvatinib and vandetanib (Supporting Information Figure S4). These data suggested that changes in the side chains at these distant sites induce conformational changes at the drug binding pocket.

Effects of the M918T mutation on drug sensitivity

The RET M918T mutation is found in the majority of sporadic MTC and is associated with the more aggressive form of MEN2B. Because the M918T mutation is prevalent in MTC, it is critical to identify RET TKIs that preferentially inhibit this mutant or that are at least as potent in inhibiting RET M918T as they are at inhibiting the wild-type RET. The M918 residue is also located in the C-lobe at a position outside of the TKI binding pocket (Figure 3A). Our findings that the V871I and F998V mutations could induce a long-range effect on drug sensitivity prompted us to examine the effect of M918T mutation on the sensitivity of these drugs.

As shown in Table 2, IC_{50}s of cabozantinib, lenvatinib, vandetanib and nintedanib in BaF3/KR (M918T) cells were 6.5-fold, 7.5-fold, 4.3-fold and 1.7-fold, respectively, higher than in BaF3/KR cells. Immunoblotting analysis showed that cabozantinib and lenvatinib were less effective in reducing pRET at the tested concentrations (Supporting Information Figure S5). We then determined the IC_{50}s of

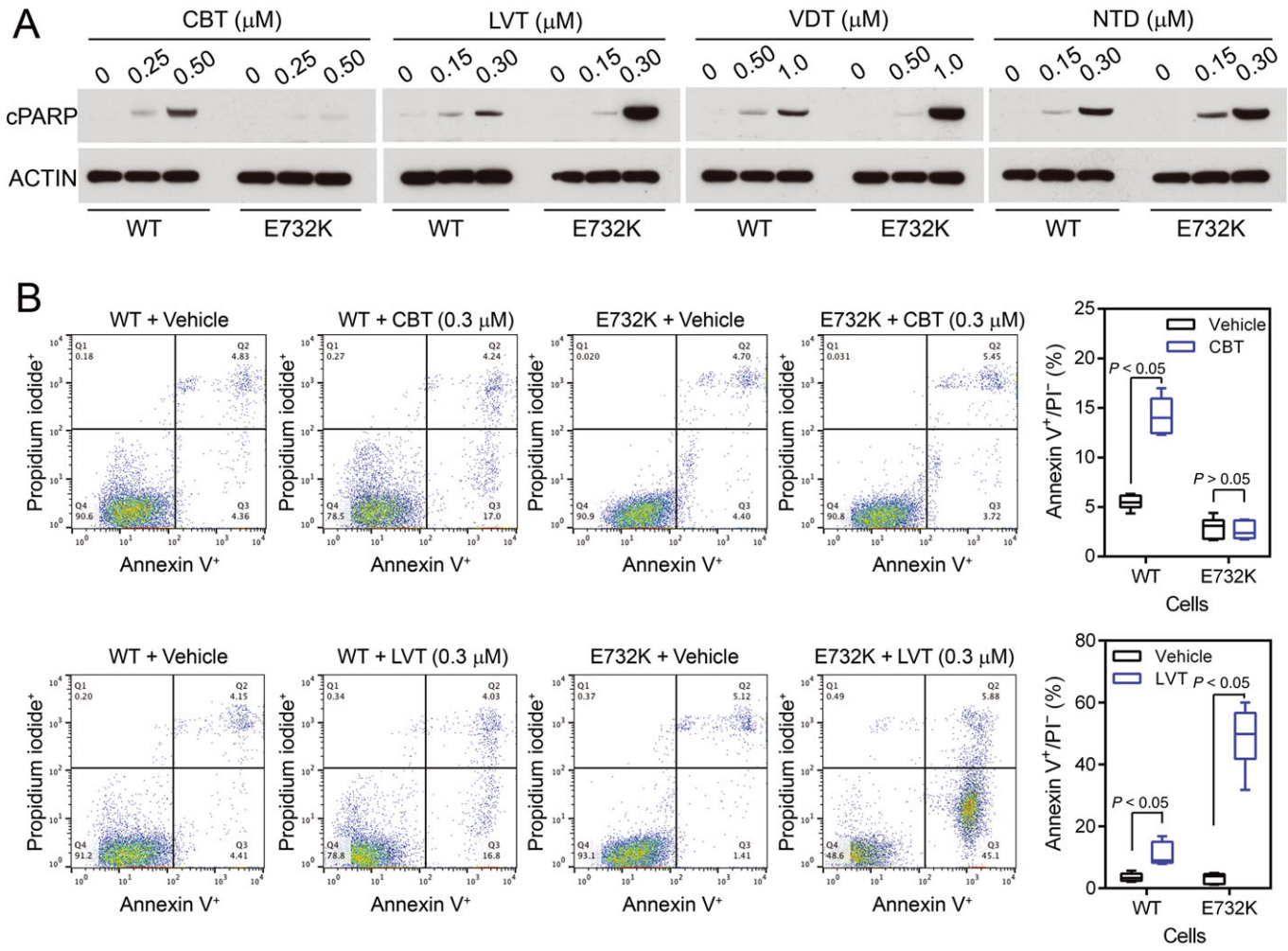

Figure 4

Comparison of apoptosis in BaF3/KR and BaF3/KR (E732K) induced by cabozantinib, lenvatinib, vandetanib and nintedanib. (A) Cells were treated with the indicated TKIs for 24 h, and cell lysates were analysed by immunoblotting with antibodies to cleaved PARP or β-actin. (B) Cells were treated with vehicle, cabozantinib or lenvatinib for 48 h, stained with annexin V/propidium iodide and analysed by flow cytometry ($n = 6$). WT, wild-type.

these compounds for the recombinant kinase domain of RET and RET (M918T) in an *in vitro* kinase assay. The *in vitro* kinase activity assays of RET and RET (M918T) were performed in parallel to minimize potential experimental variation. The results showed that the *in vitro* IC_{50}s of cabozantinib, lenvatinib, vandetanib and nintedanib for RET (M918T) kinase were 2.3-fold, 4.4-fold, 2.2-fold and 1.0-fold, respectively, of that for the wild-type RET kinase (Table 3).

For comparison, we compared the sensitivities of RET (WT), RET (V804L) and RET (V804M) kinases to nintedanib in a separate *in vitro* kinase experiment. The result showed that the V804L and V804M gatekeeper mutants had 3.6-fold and 29.9-fold, respectively, increases in nintedanib IC_{50}s (Supporting Information Figure S3).

Discussion

Missense mutations in the RET kinase domain are found in MTC and FMTC. Moreover, acquired resistance to RET kinase-targeted therapies is predicted to involve mutations in the RET kinase domain in NSCLC. In the present study, we identified mutations in the RET kinase domain that induced resistance to cabozantinib, lenvatinib, vandetanib or nintedanib, and we cross-profiled the drug sensitivity of 13 single mutants and one double mutant. The residues where mutations were identified are conserved between human and mouse RET proteins. These results provide a ready reference for the effects of these RET kinase domain mutations on the drug sensitivities of four RET TKIs.

While the four TKIs studied here had low nanomolar to subnanomolar IC_{50}s for RET or RET mutants in kinase assays *in vitro*, their IC_{50}s in BaF3/KR or BaF3/KRmut cells were >100 nM. Thus, higher concentrations of these TKIs were needed to inhibit RET phosphorylation in the cells and KR-dependent BaF3 cell survival/proliferation. The difference between IC_{50}s in *in vitro* kinase and cell-based assays may be due to higher intracellular concentration of ATP (~1 mM) than that used in the *in vitro* kinase assay

(10 μM) and other contributing factors of drug uptake/degradation in the cells.

Not surprisingly, 10 of these TKI-resistant mutations were located in the Gly-rich loop (L730, E732 and V738), the gatekeeper residue (V804) or the hinge strand (Y806, A807 and G810) that comprise approximately two-thirds of the drug binding pocket in the co-crystal structure of RET-vandetanib (PDB: 2ivu). The single-site mutants V804L, V804M and Y806C are found in patients with MEN2 and FMTC (Wells *et al*., 2013; Krampitz and Norton, 2014). We have not found mutations in the C-lobe residues that line the remaining third of the drug binding pocket. One possibility is that these residues include conserved PTK residues, such as the conserved DFG residues N-terminal to the activation loop. A change in these residues may render the kinase inactive. Another possibility is that we have not exhausted our characterization of TKI-resistant RET mutations. In fact, we only analysed a sample of the pool of random mutations of the KIF5B-RET cDNA generated in the present study. For example, a mutation at L881, a vandetanib-interacting residue, was found in FMTC (Wells *et al*., 2013). This finding suggests that the RET kinase can tolerate amino-acid substitutions at this site.

While L730I caused pan resistance to the four TKIs, L730V had a lesser effect on lenvatinib sensitivity (Table 2). Similarly, whereas G810S mutation caused pan resistance, G810A only induced resistance to vandetanib. These observations illustrate that different amino-acid substitutions of the same site could have different consequences for drug resistance. Therefore, not only the site in the kinase but also the identity of the substituting amino acid should be considered when evaluating drug sensitivity.

Although they occur less frequently, double mutations in the RET kinase domain have been observed previously (Krampitz and Norton, 2014). We identified L730V/V804M double mutations as nintedanib-resistant mutations. The nintedanib IC_{50} for the L730V/V804M double mutant (1.58 μM) was greater than the nintedanib IC_{50}s for L730V mutant (0.80 μM) and the V804M mutant (0.86 μM), indicating that the double mutation can tolerate a higher concentration of the drug.

Remarkably, two of the drug-resistant mutations that we identified (V871I and F998V) were located at distant sites in the large C-terminal lobe away from the TKI binding pocket, indicating that these mutations could exert a long-range effect on the structure of the drug binding pocket in the RET kinase domain. Significantly, we found that the prevalent MEN2B-associated RET (M918T) mutation, which is also located at a distant site in the C-lobe, also induced resistance to cabozantinib, lenvatinib and vandetanib.

A note of caution is that the RET (M918T) mutation is found in the context of full-length RET protein in MTC, whereas our data were obtained from BaF3-derived cells expressing KIF5B-RET fusion proteins and recombinant RET kinase domain proteins *in vitro*. We have not ruled out the possibility that the full-length RET and the KIF5B-RET fusion proteins or the kinase domain protein fragments may react differently towards ATP and RET kinase inhibitors.

Interestingly, a clinical trial of lenvatinib in advanced MTC found that the RET mutation status (87.5% of RET mutations in that study were M918T) did not correlate with the therapeutic response (Schlumberger *et al*., 2016). Our finding that the RET (M918T) mutant's *de novo* resistance to lenvatinib offers a potential underlying mechanism to explain this clinical observation. Significantly, we found that nintedanib was not affected by the M918T mutation or by the V871I and F998V mutations in the C-lobe. This finding raises the possibility that nintedanib may be a more effective drug for treating RET (M918T)-positive MTC.

Acknowledgements

We thank Anthony Yao, Spencer Hall, the University of Oklahoma Health Sciences Center DNA sequencing/Genomics Core staff for technical assistance and Kathy Kyler for editing the manuscript. This study was supported by the National Institutes of Health (NIH)/National Cancer Institute (NCI) grant R01CA17456 (to J.W.), a Presbyterian Health Foundation Team Science Grant (to J.W. and B.H.M.M.) and a Boehringer Ingelheim International GmbH research agreement. The shared resources at the University of Oklahoma Health Sciences Center were supported by NIH/National Institute of General Medical Sciences (NIGMS) grant P20GM103639.

Author contributions

J.W. conceived the study and contributed in the study design; X.L. and T.S. acquired the data; X.L., T.S., B.H.M.M., F.H. and J.W. analysed and/or interpreted the data; B.H.M.M. and J.W. drafted the manuscript; and X.L., T.S., B.H.M.M., F.H. and J. W. revised and approved the manuscript.

Conflict of interest

F.H. is an employee of Boehringer Ingelheim.

Declaration of transparency and scientific rigour

This Declaration acknowledges that this paper adheres to the principles for transparent reporting and scientific rigour of preclinical research recommended by funding agencies, publishers and other organisations engaged with supporting research.

References

Alexander SPH, Fabbro D, Kelly E, Marrion NV, Peters JA, Faccenda E *et al*. (2017). The Concise Guide To PHARMACOLOGY 2017/18: Catalytic receptors. Br J Pharmacol 174: S225–S271.

Cross DA, Ashton SE, Ghiorghiu S, Eberlein C, Nebhan CA, Spitzler PJ *et al*. (2014). AZD9291, an irreversible EGFR TKI, overcomes T790M-mediated resistance to EGFR inhibitors in lung cancer. Cancer Discov 4: 1046–1061.

Curtis MJ, Alexander S, Cirino G, Docherty JR, George CH, Giembycz MA *et al*. (2018). Experimental design and analysis and their

reporting II: updated and simplified guidance for authors and peer reviewers. Br J Pharmacol 175: 987–993.

Drilon A, Rekhtman N, Arcila M, Wang L, Ni A, Albano M *et al*. (2016). Cabozantinib in patients with advanced RET-rearranged non-small-cell lung cancer: an open-label, single-centre, phase 2, single-arm trial. Lancet Oncol 17: 1653–1660.

Elisei R, Schlumberger MJ, Muller SP, Schoffski P, Brose MS, Shah MH *et al*. (2013). Cabozantinib in progressive medullary thyroid cancer. J Clin Oncol 31: 3639–3646.

Gainor JF, Shaw AT (2013). Novel targets in non-small cell lung cancer: ROS1 and RET fusions. Oncologist 18: 865–875.

Gautschi O, Milia J, Filleron T, Wolf J, Carbone DP, Owen D *et al*. (2017). Targeting RET in patients with RET-rearranged lung cancers: results from the global, multicenter RET registry. J Clin Oncol 35: 1403–1410.

Gild ML, Bullock M, Robinson BG, Clifton-Bligh R (2011). Multikinase inhibitors: a new option for the treatment of thyroid cancer. Nat Rev Endocrinol 7: 617–624.

Harding SD, Sharman JL, Faccenda E, Southan C, Pawson AJ, Ireland S *et al*. (2018). The IUPHAR/BPS Guide to PHARMACOLOGY in 2018: updates and expansion to encompass the new guide to IMMUNOPHARMACOLOGY. Nucleic Acids Res 46: D1091–D1106.

Hilberg F, Roth GJ, Krssak M, Kautschitsch S, Sommergruber W, Tontsch-Grunt U *et al*. (2008). BIBF 1120: triple angiokinase inhibitor with sustained receptor blockade and good antitumor efficacy. Cancer Res 68: 4774–4782.

Hilberg F, Tontsch-Grunt U, Baum A, Le AT, Doebele RC, Lieb S *et al*. (2018). Triple angiokinase inhibitor nintedanib directly inhibits tumor cell growth and induces tumor shrinkage via blocking oncogenic receptor tyrosine kinases. J Pharmacol Exp Ther 364: 494–503.

Huang Q, Schneeberger VE, Luetteke N, Jin C, Afzal R, Budzevich MM *et al*. (2016). Preclinical modeling of KIF5B-RET fusion lung adenocarcinoma. Mol Cancer Ther 15: 2521–2529.

Johnson TW, Richardson PF, Bailey S, Brooun A, Burke BJ, Collins MR *et al*. (2014). Discovery of (10*R*)-7-amino-12-fluoro-2,10,16-trimethyl-15-oxo-10,15,16,17-tetrahydro-2*H*-8,4-(metheno) pyrazolo[4,3-*h*][2,5,11]-benzoxadiazacyclotetradecine-3-carbonitrile (PF-06463922), a macrocyclic inhibitor of anaplastic lymphoma kinase (ALK) and c-ros oncogene 1 (ROS1) with preclinical brain exposure and broad-spectrum potency against ALK-resistant mutations. J Med Chem 57: 4720–4744.

Katayama R, Lovly CM, Shaw AT (2015). Therapeutic targeting of anaplastic lymphoma kinase in lung cancer: a paradigm for precision cancer medicine. Clin Cancer Res 21: 2227–2235.

Katayama R, Shaw AT, Khan TM, Mino-Kenudson M, Solomon BJ, Halmos B *et al*. (2012). Mechanisms of acquired crizotinib resistance in ALK-rearranged lung cancers. Sci Transl Med 4: 120ra17.

Knowles PP, Murray-Rust J, Kjaer S, Scott RP, Hanrahan S, Santoro M *et al*. (2006). Structure and chemical inhibition of the RET tyrosine kinase domain. J Biol Chem 281: 33577–33587.

Kodama Y, Asai N, Kawai K, Jijiwa M, Murakumo Y, Ichihara M *et al*. (2005). The RET proto-oncogene: a molecular therapeutic target in thyroid cancer. Cancer Sci 96: 143–148.

Kohno T, Ichikawa H, Totoki Y, Yasuda K, Hiramoto M, Nammo T *et al*. (2012). KIF5B-RET fusions in lung adenocarcinoma. Nat Med 18: 375–377.

Kohno T, Nakaoku T, Tsuta K, Tsuchihara K, Matsumoto S, Yoh K *et al*. (2015). Beyond ALK-RET, ROS1 and other oncogene fusions in lung cancer. Transl Lung Cancer Res 4: 156–164.

Kohno T, Tsuta K, Tsuchihara K, Nakaoku T, Yoh K, Goto K (2013). RET fusion gene: translation to personalized lung cancer therapy. Cancer Sci 104: 1396–1400.

Krampitz GW, Norton JA (2014). RET gene mutations (genotype and phenotype) of multiple endocrine neoplasia type 2 and familial medullary thyroid carcinoma. Cancer 120: 1920–1931.

Mulligan LM (2014). RET revisited: expanding the oncogenic portfolio. Nat Rev Cancer 14: 173–186.

Mulligan LM (2016). Progress and potential impact of RET kinase targeting in cancer. Expert Rev Proteomics 13: 631–633.

Pasini A, Geneste O, Legrand P, Schlumberger M, Rossel M, Fournier L *et al*. (1997). Oncogenic activation of RET by two distinct FMTC mutations affecting the tyrosine kinase domain. Oncogene 15: 393–402.

Plaza-Menacho I, Barnouin K, Goodman K, Martinez-Torres RJ, Borg A, Murray-Rust J *et al*. (2014). Oncogenic RET kinase domain mutations perturb the autophosphorylation trajectory by enhancing substrate presentation in trans. Mol Cell 53: 738–751.

Riely GJ, Yu HA (2015). EGFR: The Paradigm of an Oncogene-Driven Lung Cancer. Clin Cancer Res 21: 2221–2226.

Roth GJ, Binder R, Colbatzky F, Dallinger C, Schlenker-Herceg R, Hilberg F *et al*. (2015). Nintedanib: from discovery to the clinic. J Med Chem 58: 1053–1063.

Roth GJ, Heckel A, Colbatzky F, Handschuh S, Kley J, Lehmann-Lintz T*et al*. (2009). Design, synthesis, and evaluation of indolinones as triple angiokinase inhibitors and the discovery of a highly specific 6-methoxycarbonyl-substituted indolinone (BIBF 1120). J Med Chem 52: 4466–4480.

Sabari JK, Santini FC, Schram AM, Bergagnini I, Chen R, Mrad C *et al*. (2017). The activity, safety, and evolving role of brigatinib in patients with ALK-rearranged non-small cell lung cancers. Onco Targets Ther 10: 1983–1992.

Schlumberger M, Jarzab B, Cabanillas ME, Robinson B, Pacini F, Ball DW*et al*. (2016). A phase II trial of the multitargeted tyrosine kinase inhibitor lenvatinib (E7080) in advanced medullary thyroid cancer. Clin Cancer Res 22: 44–53.

Schlumberger M, Tahara M, Wirth LJ, Robinson B, Brose MS, Elisei R *et al*. (2015). Lenvatinib versus placebo in radioiodine-refractory thyroid cancer. N Engl J Med 372: 621–630.

Scott LM, Chen L, Daniel KG, Brooks WH, Guida WC, Lawrence HR *et al*. (2011). Shp2 protein tyrosine phosphatase inhibitor activity of estramustine phosphate and its triterpenoid analogs. Bioorg Med Chem Lett 21: 730–733.

Shen T, Chen Z, Zhao ZJ, Wu J (2017). Genetic defects of the IRF1-mediated major histocompatibility complex class I antigen presentation pathway occur prevalently in the JAK2 gene in non-small cell lung cancer. Oncotarget 8: 60975–60986.

Sherman SI, Clary DO, Elisei R, Schlumberger MJ, Cohen EE, Schoffski P *et al*. (2016). Correlative analyses of RET and RAS mutations in a phase 3 trial of cabozantinib in patients with progressive, metastatic medullary thyroid cancer. Cancer 122: 3856–3864.

Song M (2015). Progress in discovery of KIF5B-RET kinase inhibitors for the treatment of non-small-cell lung cancer. J Med Chem 58: 3672–3681.

Takeuchi K, Soda M, Togashi Y, Suzuki R, Sakata S, Hatano S *et al*. (2012). RET, ROS1 and ALK fusions in lung cancer. Nat Med 18: 378–381.

Wells SA Jr, Pacini F, Robinson BG, Santoro M (2013). Multiple endocrine neoplasia type 2 and familial medullary thyroid carcinoma: an update. J Clin Endocrinol Metab 98: 3149–3164.

Wells SA Jr, Robinson BG, Gagel RF, Dralle H, Fagin JA, Santoro M *et al*. (2012). Vandetanib in patients with locally advanced or metastatic medullary thyroid cancer: a randomized, double-blind phase III trial. J Clin Oncol 30: 134–141.

Yakes FM, Chen J, Tan J, Yamaguchi K, Shi Y, Yu P *et al*. (2011). Cabozantinib (XL184), a novel MET and VEGFR2 inhibitor, simultaneously suppresses metastasis, angiogenesis, and tumor growth. Mol Cancer Ther 10: 2298–2308.

Yoh K, Seto T, Satouchi M, Nishio M, Yamamoto N, Murakami H *et al*. (2017). Vandetanib in patients with previously treated RET-rearranged advanced non-small-cell lung cancer (LURET): an open-label, multicentre phase 2 trial. Lancet Respir Med 5: 42–50.

Zou HY, Friboulet L, Kodack DP, Engstrom LD, Li Q, West M *et al*. (2015). PF-06463922, an ALK/ROS1 inhibitor, overcomes resistance to first and second generation ALK inhibitors in preclinical models. Cancer Cell 28: 70–81.

Supporting Information

Additional supporting information may be found online in the Supporting Information section at the end of the article.

https://doi.org/10.1111/bph.14395

Figure S1 Comparison of RET mutants expressed in stable BaF3 derived cell lines. Cell lysates of indicated cell lines were prepared and equal amounts of protein were analyzed by immunoblotting with antibodies to the Flag-tag or actin.

Figure S2 Comparison of sensitivities to vandetanib between BaF3/RET (G810S) and two vandetanibresistant BaF3/RET (G810S/G949R) cell lines. Experiments were performed as described in the Methods section of the main text.

Figure S3 Comparison of inhibiting RET, RET (V804L), and RET (V804M) kinase activity by nintedanib *in vitro*. The *in vitro* kinase assay was performed as a commercial service by Reaction Biology (Malvern, PA) in parallel 10-dose IC50 singlet assay, with 3-fold serial dilution starting at 10 μM. Curve fitting was as described (Scott *et al*., 2011).

Figure S4 Immunoblot analysis of pRET in BaF3/KR, BaF3/KR (V871I), and BaF3/KR (F998V) cells after TKI treatment. (A) BaF3/KR and BaF3/KR (V871I) cells were treated with cabozantinib, lenvatinib, or vandetanib at the indicated concentrations for 4 h. Cleared cell lysates were analyzed by immunoblotting with indicated antibodies. (B) BaF3/KR and BaF3/KR (F998V) cells were treated and analyzed as in (A).

Figure S5 Inhibition of KR and KR (M918T) kinase activities in BaF3/KR and BaF3/KR (M918T) cells by cabozantinib, lenvatinib, vandetanib, and nintedanib. Cells were treated with 0, 0.1, or 0.25 μM of each TKI for 4 h (A) or with the indicated concentration of vandetanib for 4 h (B). Cell lysates were analyzed by immunoblotting with antibodies to pRET or flag-tag.

Table S1 KIF5B-RET mutations in nintedanib-resistant cell lines derived from BaF3/KR cells*.